E1-2001-157

TIME SCALE
OF THE THERMAL MULTIFRAGMENTATION
IN $p + \mathrm{Au}$ COLLISIONS AT 8.1 GeV

Submitted to «Nuclear Physics A»

V.K.Rodionov[1], S.P.Avdeyev, V.A.Karnaukhov, L.A.Petrov, V.V.Kirakosyan, P.A.Rukoyatkin
Joint Institute for Nuclear Research, 141980, Dubna, Russia

H.Oeschler
Institute fur Kernphysik, TU Darmstadt, 64289, Germany

A.Budzanowski, W.Karcz, M.Janicki
H.Niewodniczanski Institute of Nuclear Physics, 31-342, Cracow, Poland

O.V.Bochkarev, E.A.Kuzmin, L.V.Chulkov
Kurchatov Institute, 123182, Moscow, Russia

E.Norbeck
University of Iowa, Iowa City, IA 52242, USA

A.S.Botvina[2]
GSI, Postfach 110552, D-64220 Darmstadt, Germany

[1]E-mail: radionov@nusun.jinr.ru
[2]On leave from the INR, Moscow

1. Introduction

Nuclear multifragmentation is a new decay mode of highly excited nuclei in which several intermediate mass fragments (IMF, $3 \leq Z \leq 20$) are emitted. A recent review can be found in Ref. [1]. This process is actively investigated now by means of different 4π–setups. There are two ways of creating the very excited nuclei: heavy ion collisions at intermediate energies and reactions with light relativistic projectiles. In the last case the decay process is hardly influenced by the compression, fast rotation or shape distortion of the fragmenting system, which occurs with heavy ion collisions. The excitation energy is expected to be almost thermal. So, that provides a unique chance to study thermal multifragmentation, for which the decay properties of a target spectator are governed in the main by the nuclear heating. It has been already proved in a number of papers (see for example Ref. [2–11]), that thermal multifragmentation indeed takes place in collisions of relativistic protons, ^4He, ^3He, antiprotons and pions with heavy targets.

The time scale of fragment emission is a key point for understanding this decay mode. Is it a sequential process of independent evaporation of IMF's, or a new multi–body decay mode with "simultaneous" emission of fragments governed by the total accessible phase space? As it was suggested in Ref. [12], "simultaneous" means that the primary fragments are liberated at freeze–out during a time interval that is smaller than the Coulomb interaction time $\tau_c \approx 10^{-21}$ s (300–400 fm/c). In that case fragment emissions are not independent as they interact via Coulomb forces while accelerating in the common electric field. So, measuring the IMF emission time τ_{em} (i.e. the mean time interval between sequential fragment emissions), or the mean life time τ of fragmenting system is a direct way to answer the question about the nature of the multifragmentation phenomenon. There is a simple relation between these two quantities via the mean IMF multiplicity [13,14].

Two procedures are used to determine the time scale of the process: analysis of the IMF–IMF correlation function in respect to the relative angle or the relative velocity. The correlation function exhibits a minimum at $\Theta_{rel} = 0$ ($\nu_{rel} = 0$) arising from the Coulomb repulsion between the coincident fragments. The magnitude of this effect depends drastically on the mean emission time, since the longer the time separation of the fragments, the larger their space separation and the weaker the Coulomb repulsion. The time scale for IMF emission is estimated by comparing the measured correlation function to that obtained by the multibody Coulomb trajectory calculations with τ (or τ_{em}) as a parameter. A short review of the data on the IMF emission times is given in [15] for the collisions induced by different projectiles [16–22]. It is shown that for beam energies higher than 1.5 GeV the measured τ are less than τ_c and that is in a favor of a true multifragmentation mechanism. Systematics of the fragment emission times as a function of the excitation energy is given in [23]. It indicates that τ falls down very fast in the range 2–4 MeV/nucleon reaching the values $\tau \leq 75$ fm/c.

The first time scale measurements for the thermal multifragmentation have been done in [13,14] for $^4He + Au$ collisions at 14.6 GeV by analyzing the IMF–IMF relative angle correlation. It was found that τ is less than 75 fm/c. Later on a breakup time of order (20–50) fm/c was estimated via small–angle IMF–IMF relative velocity correlations for $^3He + Au$ interactions at 4.8 GeV [22].

In this paper the data on the time scale measurements for the multi–fragment emission in $p + Au$ collisions at 8.1 GeV are presented in addition to the detailed analysis of that process given in Ref. [5,11]. Emphasis is put on the question of the model dependence of the results obtained.

2. Data sampling

The experiment has been performed with the 4π—setup FASA [24] installed at the beam of the Dubna synchrophasotron. The device consists of two main parts:

1) Five $dE - E$–telescopes (at $\Theta = 24°$, $68°$, $87°$, $112°$ and $156°$ to the beam direction), which serve as triggers for the read–out of the system allowing the measurement of the fragment charge and energy distributions. The ionization chambers and Si(Au)–detectors are used respectively as dE and E counters.

2) The fragment multiplicity detector (FMD) including 64 CsI(Tl) counters (with a scintillator thickness averaging 35 mg $\cdot$ cm^{-2}), which cover 89% of 4π. The FMD gives the number of IMF's in the event and their angular distribution.

A self–supporting Au target 1.0 mg/cm^2 thick is located in the center of the FASA vacuum chamber. The beam intensity was around $7 \cdot 10^8$ p/spill (spill length – 300 ms, spill period – 10 s).

The response function of the CsI(Tl) was calculated from empirical data [24]. The pulse–height thresholds were set off–line for each counter individually, depending on the scintillator thickness, to get the admixture of lighter particles ($Z = 1$ and 2) of about 5% to the counting rate of IMF's. As a result the detection threshold of

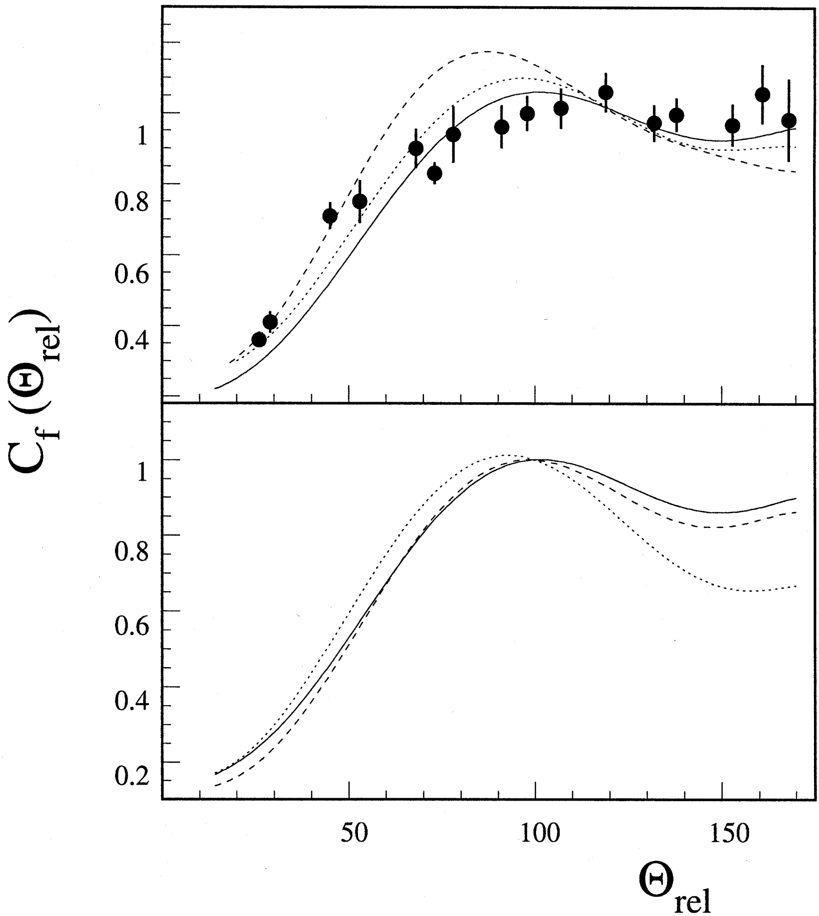

Fig.1. Upper panel: Relative angle correlation function for IMF produced in $p + Au$ collisions at 8.1 GeV. The lines are calculated for prompt IMF emission with RC+α+SMM (solid and dashed) and RC+α_0+SMM (dotted) models under two assumptions about the mean time of secondary disintegration: $\tau_{sd} \ll \tau_c$ (dashed line) and $\tau_{sd} > \tau_c$. Lower panel: The evolution of the calculated $C_f(\Theta_{rel})$ while the different ingredients of the "experimental filter" are applied: dotted line –energy threshold (2 MeV/nucleon) is introduced, dashed line – normalization to the angular distribution with respect to the beam direction, solid line – smoothing to take into account the angular acceptance of the scintillators.

CsI(Tl) for IMF's was chosen to be around 2 MeV/nucleon. Under this condition, detection of Li with an energy higher than 12 MeV/nucleon is excluded, while there is no high energy cut–off for the detection of heavier fragments. The mean charge of IMF's detected by the FMD is estimated to be ≈ 6.5.

To study the IMF–IMF correlation as a function of their relative angle, the coincidence yields have been measured for the trigger telescopes i and scintillator counters k: $dY_i(\Theta_{ik})/d\Omega_k = Y_{ik}$. The correlation function $C_f(\Theta_{rel})$ is defined as the ratio of Y_{ik} to the counting rate in the same scintillator k, but triggered by the "remote" telescope j, for which $\Theta_{jk} > 90°$. Both counting rates are reduced by the number of triggering counts and the contributions of different telescopes i are summed:

$$C_f(\Theta_{rel}) = C \sum Y_{ik}(\Theta_{ik}) \cdot \frac{N_j}{N_i Y_{jk}} \tag{1}$$

where $i = 1-5$, $k = 1-64$ and C is a constant. In fact the number of significantly different relative angles Θ_{ik} is remarkably smaller than the total number of pairs. The data for the close values of the relative angles are summed and reduced to the unique solid angle. Note that the normalization in that formula eliminates the deviations in the efficiency of the telescopes and scintillators and compensates the influence of the angular anisotropy with respect to the beam direction.

The experimental correlation function for the intermediate mass fragments from $p + Au$ collisions at 8.1 GeV is shown in Fig. 1 (upper panel). Those events have been separated for which IMF's with $Z \geq 6$ are detected by the telescopes. This condition was imposed to minimize the influence of the preequilibrium emission (which probably takes place for Li and Be) and to enlarge the suppression of the small relative angle yield. This suppression is apparent in the data. The statistical multifragmentation model (SMM) [25] is used in the analysis of the correlation functions. Together with data, Fig.1 presents also some examples of calculated $C_f(\Theta_{rel})$ (for prompt fragment emission) folded with the experimental filter illustrated in lower panel (see later for details).

3. Thermal multifragmentation and SMM

The reaction induced by a light relativistic projectile is usually divided into two steps. The first is a fast energy–deposition stage, during which energetic light particles are emitted leaving an excited nuclear remnant (target spectator). The second is the statistical decay of this remnant. We used a refined version of the

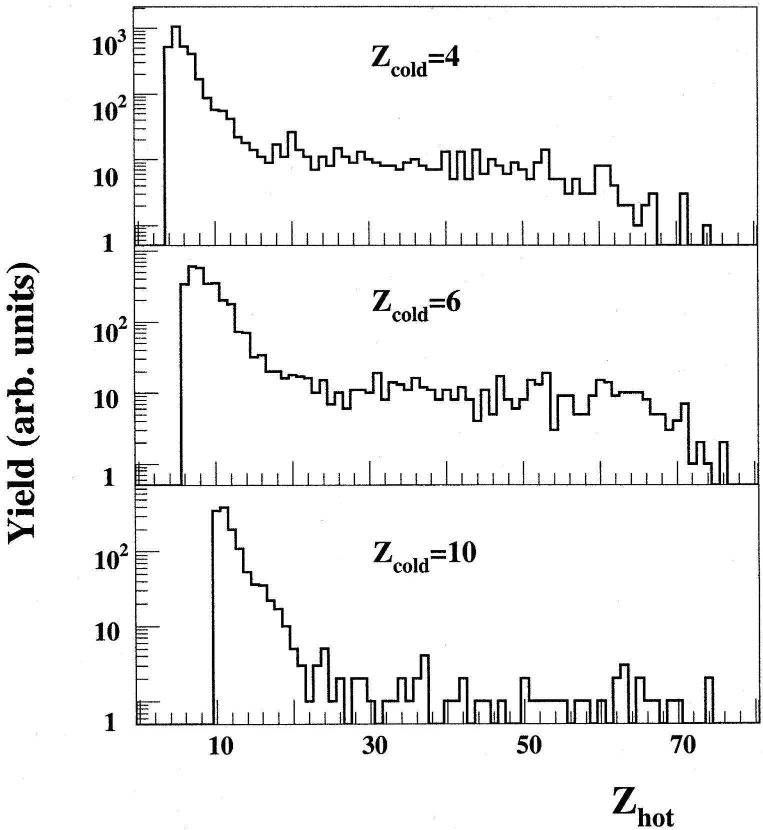

Fig.2. The calculated distributions of hot primary prefragments which give the cold fragments with $Z = 4,\ 6$ and 10 after deexcitation.

intranuclear cascade model (RC) [26,27] to get the distributions of the target spectators over A, Z and the excitation energy. The second stage is described by SMM. Within the statistical multifragmentation model the probability of the equilibrium decay into a given channel is proportional to its statistical weight. The break–up volume determining the Coulomb energy of the system is a key parameter of the model. It is taken as $V_b = (1 + k)A/\rho_o$, where A is the mass number of the fragmenting nucleus, ρ_o is the normal nuclear density and k is a free parameter. It was demonstrated already in a number of papers that the break–up of the hot system occurs after its expansion to a density $\rho_b \leq 1/3\rho_o$ driven by the thermal pressure. In this paper $k = 3$ is used (i.e. $V_b = 4V_o$), which is more adequate for simultaneous description of the fragment multiplicity, charge and kinetic energy distributions.

The primary fragments are hot and their deexcitation is considered by SMM to get the final distributions of cold IMF's. It is usually assumed that this secondary decay occurs just after the acceleration of the hot fragments in the Coulomb field of the source. Fig.2 illustrates the significance of this process. It presents the calculated charge distributions of the hot precursors for the final cold fragments with $Z = 4$, 6, 10. Each distribution has a prominent peak close to these Z values followed by a long tail due to the IMF evaporation from the excited residuals of the spallation process. Later we shall analyze how the correlation function is sensitive to the assumptions on the mean time for the secondary decay.

The model calculations (RC+SMM) fail to describe the data for the IMF multiplicities [5,11]. One concludes that the cascade calculation overestimates the high energy tail of the residue excitation energy distribution $f(E_{RC})$, which results in the overprediction of the mean IMF– mulitiplicitiy $< M >$: the calculated value is equal to 3.58, while the measured one is 2.1 ± 0.2 (for the events with at least one IMF). In order to overcome this difficulty two empirical modifications of $f(E_{RC})$ are suggested in [5]. The first is the simple reduction of E_{RC} by a factor $\alpha < 1$ on an event by event basis. It is motivated by the idea that the "frozen mean field" approximation in the cascade calculation may lead to an overestimation of the high energy part of the energy distribution which plays a crucial role in fragment formation. This modified model is denoted as RC+α_0+SMM (α_0 for short). Another recipe for "improving" the model is the simultaneous modification of the excitation energies and masses of the residual nuclei: E_{RC} is reduced by the factor α, while the remnant mass number (as well as its Z value) is decreased by a value that is proportional to the mass loss in the cascade: $\Delta A = \beta \cdot \Delta A_{RC}$. It is motivated that $\beta \approx (1 - \alpha)$ [5]. This change takes into account effectively the possible mass and energy loss due to the preequilibrium emission and particle evaporation during the expansion stage (in the spirit of the EES model [28]). In both approaches, the parameter α is adjusted to get the mean multiplicity close to the measured one. The second approach is denoted as RC+α+SMM (α for short) and it seems to be more motivated physically. Table 1 gives the calculated properties of the residual nuclei from $p + Au$ collisions at 8.1 GeV. The parameter α is equal to 0.60 in first model and 0.53 in the second one.

The experimental data on the fragment multiplicity and charge distributions as well as the fragment kinetic energy spectra are described almost equally well by RC+α_0+SMM and RC+α+SMM codes, therefore the both combined model should be used in the calculation of the correlation function. Note that the mean excitation energies for both systems (for $M \geq 2$) are estimated to be ~ 4.0 MeV/nucleon.

An important part of the SMM is a calculation of the multibody Coulomb trajectories, which starts with placing all of the charged particles of a given partition inside the break–up volume. Each particle is assigned a thermal momentum corresponding to the system temperature. To avoid the overlapping of fragments $V_b = 8V_o$ is used in this part of the calculation. The resulting values of the kinetic energies are finally corrected (by factor η, according to the energy conservation law) to the right Coulomb energy of the system with $V_b = 4V_o$ [25].

Table 1. *The calculated properties of fragmenting nuclei produced in $p + Au$ collisions at 8.1 GeV: M is the IMF multiplicity, $Z_{M\geq1}$, $A_{M\geq1}$, and $A_{M\geq2}$ are the mean charge and mass numbers of the fragmenting source, $E_{M\geq1}$ and $E_{M\geq2}$ are the mean excitation energies (in MeV) corresponding to fragment emission with $M \geq 1$ and $M \geq 2$ respectively.*

$< M >$	$Z_{M\geq1}$	$A_{M\geq1}$	$A_{M\geq2}$	$E_{M\geq1}$	$E_{M\geq2}$	Model
3.9	73	175	173	806	901	RC+SMM
2.16	67	157	153	524	608	RC+α+SMM
2.05	72	172	168	582	690	RC+α_0+SMM

One should note that this normalization does not change the directions of IMF–momentum and fragment trajectories are left unchanged in fact, giving reduced effect of the small angle suppression. The importance of this point for the time scale estimation will be considered later.

The Coulomb trajectory calculations are followed for 3000 fm/c. After this amount of time the fragment kinetic energy is close to its asymptotic value. This is demonstrated in Fig.3 where the mean energies of Be, C and Mg are shown as a function of t_{acc} – the time interval after the start of the acceleration. The characteristic Coulomb time τ_c is marked corresponding to the moment when the fragments reach 90% of their final energy. It is seen from Fig.3 that the largest part of the IMF kinetic energy is Coulomb in origin. The thermal part is about 10 MeV.

The mean fragment energy per nucleon [5] is shown in Fig.4 as a function of fragment charge. The solid line is calculated by the combined model RC+α+SMM.

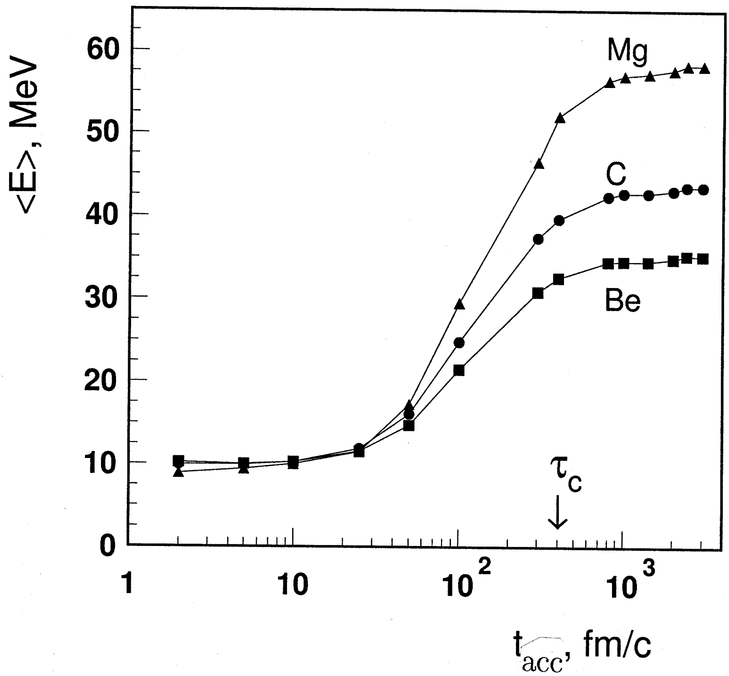

Fig.3. The calculated mean kinetic energies of Be, C and Mg as a function of the time interval after the start of acceleration t_{acc}.

The data are close to the calculated values for $Z = 4-9$. The deviation for heavier fragments is interpreted in [5] as an indication on the preferential location of the heavier fragments in the interior of the freeze out volume. The lower line (dot–dashed) is obtained by the calculation of the Coulomb trajectories for a break up volume of $8V_o$ (without the correction mention above) and that in fact is used for composing the correlation function. One can imagine that the actual starting configuration for the Coulomb expansion from the break–up volume $V_b = 4V_o$ is composed by closely packed and properly deformed fragments. To model this situation the following procedure is used: fragments are placed in $V_b = 8V_o$ without overlapping, then their centers are rescaled according to real break–up volume $4V_o$ and the Coulomb trajectory calculations are performed for the point like particles (note, that zero distance between fragments centers is excluded). The dotted line above the data is obtained for that case by the RC+α+SMM approach. Note that correcting the results by factor η reduces the energies to be very close to the solid line. The dashed line is calculated with RC+α_0+SMM. It is slightly above the solid line as the mean charge of fragmenting nucleus is larger than in the previous case.

4. Comparison between experimental data and model

For the model calculation of the correlation function those generated events have been selected for which the IMF multiplicity is $M \geq 2$ and at least one fragment has $Z \geq 6$. The "experimental filter" was applied to be in the line with the experimental definition of the correlation function (1). This is illustrated by Fig.1 (lower panel) for the case of the prompt fragment emission ($\tau = 0$). First of all, only fragments with the energy $E \geq 2$ MeV/nucleon were used in the calculations (dotted line). To eliminate the fragment momentum bunching by the source velocity, the coincidence yield $Y_{ik}(\Theta_{ik})$ was normalized on $W(\Theta_k)$ on an event by event basis, where $W(\Theta)$ is the IMF angular distribution with respect to the beam direction. The result is shown by dashed line. Finally, the correlation function has been smoothed properly to take into account the angular acceptance of the scintillators, which is equal to $\delta = \pm 12°$. This was done by numerical integration (solid line) :

$$Y(\Theta_{rel}) = B \int_{\Theta_{rel}-\delta}^{\Theta_{rel}+\delta} Y(\Theta_{12}) d\Theta_{12} \qquad (2)$$

Now let us return to upper panel of Fig.1 where three model correlation functions (for prompt emission) are compared. First of all the calculations have been performed with RC+α+SMM model under two assumptions about the mean secondary disintegration time τ_{sd} for the fragments: very short, $\tau_{sd} \ll \tau_c$, and larger than the time of acceleration ($\tau_{sd} > \tau_c$). In the first case (dashed line) the cold fragments are accelerated, interacting with each other via Coulomb forces. In the second variant (solid line) the primary excited fragments (with higher charges) propagate through the Coulomb field. One might expect very different correlation patterns. But the resulting curves deviate not so much from each other.The calculation with the RC+α_0+SMM approach and $\tau_{sd} > \tau_c$ (dotted line) gives similar results. This indicates that some ambiguity (within 10%, see Table 1) in the knowledge of charges (masses) and excitation energies of the fragmenting nuclei is not so important.

Composing the correlation function for the different mean decay times of the system has been performed for all the models and assumptions mentioned above.

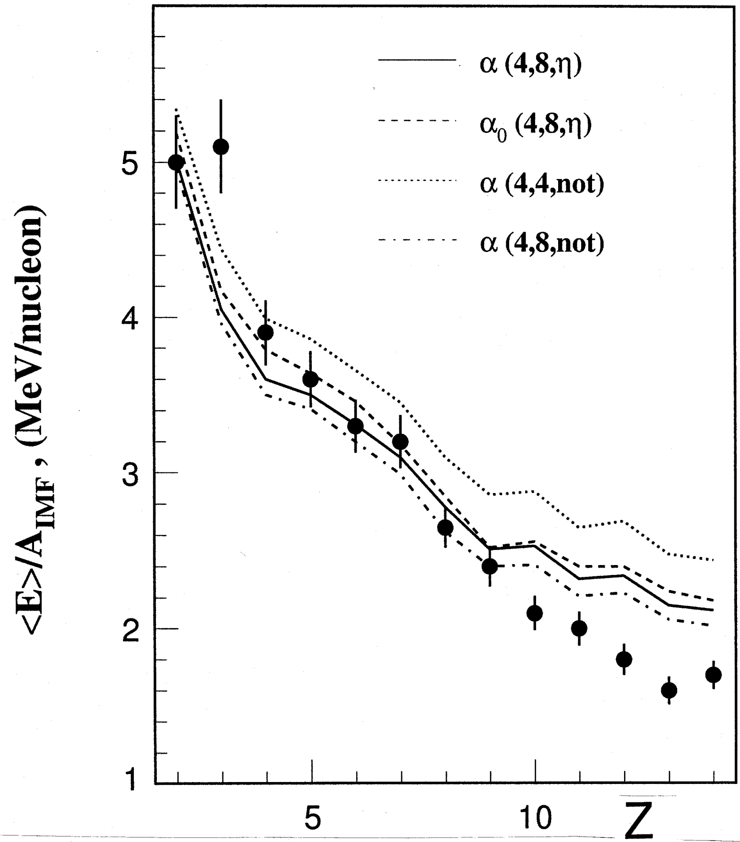

Fig.4. Mean fragment energies per nucleon as a function of the fragment charge. Full circles are the experimental data. The lines are calculated with RC+α+SMM and RC+α_0+SMM under different assumptions. The first number in the brackets is V_b/V_0 used in the partition calculations, the second one is the system volume (relative to V_0) at the beginning of the Coulomb expansion; η symbolizes the energy correction to the right Coulomb energy of the system.

For each fragment in a given event the starting time to move along a Coulomb trajectory has been randomly chosen according to the decay probability of the system: $P(t) \sim exp(-t/\tau)$. The calculations were done for $\tau = 0,\ 50,\ 100,$ and 200 fm/c. The upper panel of Fig.5 shows the results obtained with RC+α+SMM, assuming $k = 3$ and $\tau_{sd} > \tau_c$. Both the data and the model correlation function are fitted to unity by the least–squares method in the range $\Theta_{rel} > 90°$.

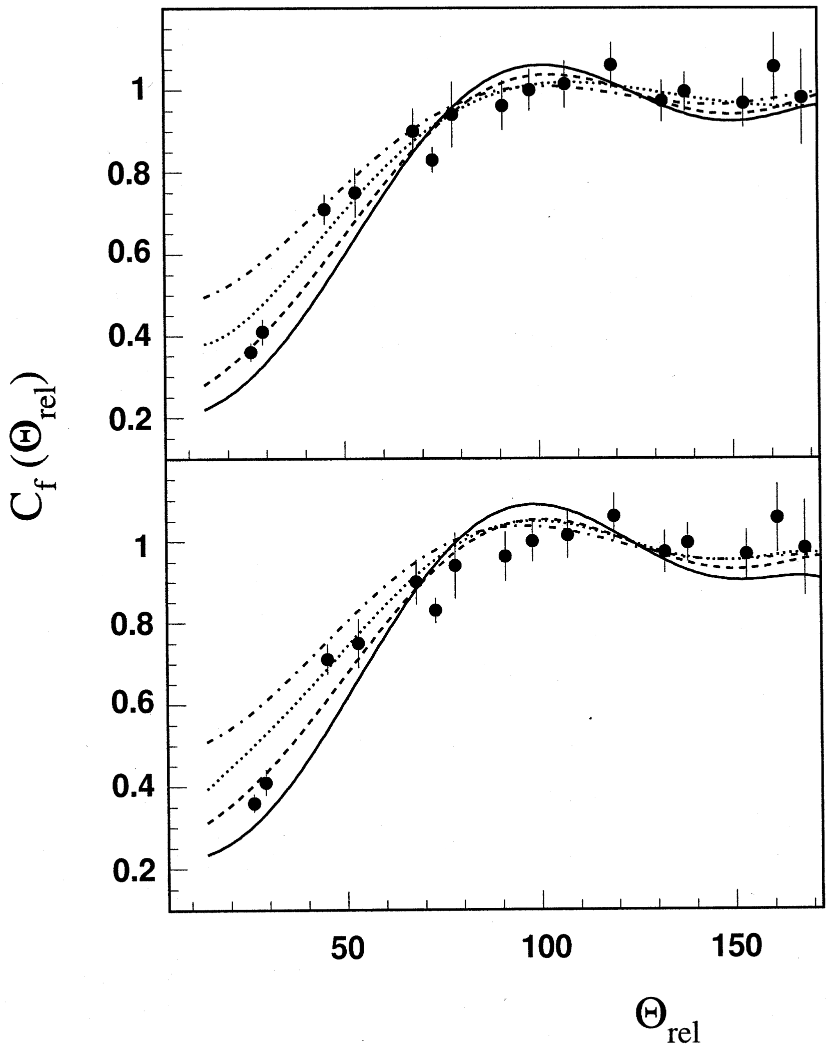

Fig.5. Comparison of the measured correlation functions (full circles) with the calculated ones for different mean decay times of the fragmenting system: solid, dashed, dotted and dash – dotted lines for $\tau = 0,\ 50,\ 100$ and 200 fm/c. The upper panel is for the RC+α+SMM model with the parameters $(4, 8, \eta)$ (see notation in Fig.4) , the lower panel is for the same model, but with the parameters $(4, 4, \eta)$ allowing the fragments to overlap (see text).

As it mentioned above, the trajectory calculations in that case are made for the break up volume $8V_o$, i.e. under conditions of reduced Coulomb field in comparison to that for the claimed value of the model parameter k. How are results changed with a decrease of the system volume at the beginning of Coulomb expansion? To estimate this change the correlation function was calculated using the Coulomb trajectories for $V_b = 4V_o$, assuming point like fragments (see the end of the previous chapter). The result is shown in the lower panel of Fig.5 : suppression of the small angle yield becomes only slightly weaker because of some compensating effects.

As the measure of the IMF–IMF repulsion effect, the ratio of the correlation function values at $\Theta_{rel} > 90°$ (the mean value) and at $\Theta_{rel} = 26°$ is used. This quantity is shown in Fig.6 as a function of τ, the mean life time of the system. The calculations have been done by the models discussed above: by RC+α+SMM under two assumption for the probability of the secondary decay, with RC+α_0+SMM, and for point like fragments. The crossing of the obtained lines with the band corresponding to the measured ratio and its error bar ($\pm 2\sigma$) defines the mean life time of fragmenting nuclei produced in $p + Au$ collisions at 8.1 GeV. The results obtained with different model assumptions are presented in Table 2 and they are in agreement with the systematic set of the data for the reactions of energetic hadrons with Au given in [29].

Table 2. *The mean decay time of the fragmenting system obtained by analysis of the measured IMF–IMF correlation function. Notation is the same as in Figs.4 and 5.*

Model	$\alpha(4,8,\eta)$	$\alpha(4,4,\eta)$	$\alpha(4,8,\eta)$ cold	$\alpha_0(4,8,\eta)$
τ, fm/c	50 ± 18	37 ± 13	27 ± 17	≤ 45

It is crucially important in this analysis to have confidence in the code for the multibody Coulomb trajectory calculations. To control that point we performed also the calculations using the very different approach developed in the paper [30] by Dubna mathematicians: no significant deviations from the results presented above were found.

As it already mentioned, the SMM overpredicts the mean kinetic energies of the heavier IMF's. How does this influence on the time scale estimation? It was found that a softening of the energy spectra of fragments with $Z > 9$ produces a decrease in the depth of the Coulomb well. It means that using the more correct

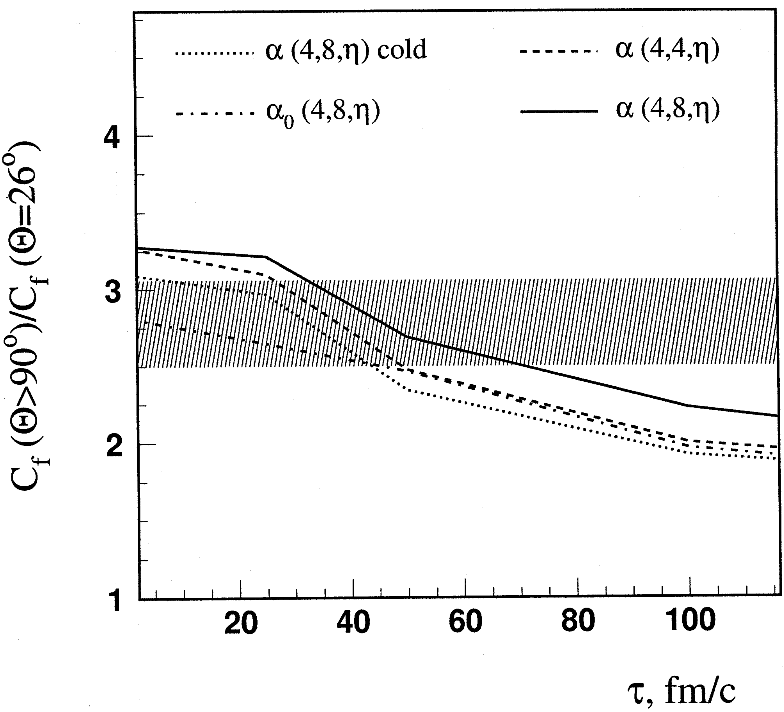

Fig.6. Ratio of the correlation function at $\Theta_{rel} > 90^\circ$ to that at $\Theta_{rel} = 26^\circ$ versus the mean decay time of the system. The experimental value is given by the horizontal band, the lines are calculated using different models as discussed in the text. Notation is the same as in Fig.4. Only calculations given by the dotted line are made assuming very fast secondary disintegration of fragments ("cold" acceleration).

kinetic energies for the heavier IMF's might result in slightly smaller values for τ. We come to a similar conclusion considering the influence of the admixture ($\sim 5\%$) of helium to the counting rate of IMF's: this admixture gives rise a slight increase of the measured fragment emission time.

5. Conclusion

The distribution of relative angles between the intermediate mass fragments has been measured and analyzed for the first time for thermal multifragmentation in $p + Au$ collisions at 8.1 GeV. The analysis has been done on an event by event basis. The multi-body Coulomb trajectory calculations of all charged particles have been performed starting with the initial break–up conditions given by the combined model with the revised intranuclear cascade (RC) followed by the statistical multifragmentation model. The distributions of the excitation energy and residual masses after RC has been empirically modified to take into account the expansion stage and to reach agreement with the data for the mean IMF multiplicity. The correlation function was calculated for different values of τ, the mean life time of the system, and compared with the measured one to find the actual time scale of the IMF emission. Emphasis was put on the model dependence of the results obtained: a) two variants of the combined model have been used for which the properties of the fragmenting nuclei are different; b) dependence of the results on the instant of the secondary decay of the hot primary fragment was controlled; c) the sensitivity of the shape of correlation function on the size of the break–up volume was checked. It was found that the measured mean life time of the system is always $\tau \leq 70$ fm/c, which is in accordance with the scenario of a "simultaneous" multi-body decay of a hot and expanded nuclear system.

Acknowledgements

The authors are thankful to Profs. A.Hrynkiewicz, S.T.Belyaev, A.I.Malakhov, N.A.Russakovich for support and to the staff of the JINR synchrophasotron for running the accelerator. The research was supported in part by Grant No 00–02–16608 from the Russian Foundation for Basic Research, by Grant of Polish Plenipotentiary in JINR, by Grant NATO PST.CLG.976861, by Grant No1P03 12615 from the Polish State Committee for Scientific Research, by Contract No 06DA453 with Bundesministerium fuer Forschung und Technologie and by the US National Science Foundation.

References

1. "Multifragmentation", Proc. of Int. Workshop XXVII on Gross Properties of Nuclei and Nuclear Excitations, Hirschegg, Austria, Jan. 17–23, 1999. Edited by H.Feldmeier, J.Knoll, W.Norenberg, J.Wambach. GSI, Darmstadt, 1999.

2. V.V.Avdeichikov, et al. Yad.Fiz., **48** (1988) 1796.

3. S.J.Yennello, et al. Phys.Rev.Lett., **67** (1991) 671.

4. Bao–An Li, D.H.E.Gross, V.Lips, H.Oeschler. Phys.Lett., **B335** (1994) 1.

5. S.P.Avdeyev, et al. JINR Rapid Communications **2[82]** (1997) 71;
S.P.Avdeyev, et al. Eur.Phys.J., **A3** (1998) 75.

6. K.Kwiatkowski, et al. Phys.Rev.Lett., **74** (1995) 3756.

7. K.H.Tanaka, et al. Nucl.Phys., **A583** (1995) 581;
T.Murakami, et al. KEK Preprint 2000–40, Tsukuba (2000).

8. E.R.Foxford, et al. Phys.Rev., **C54** (1996) 749.

9. L.Beaulieu, et al. Phys.Lett., **B463** (1999) 159.

10. F.Goldenbaum, et al. Phys.Rev.Lett., **77** (1996) 1230.

11. S.P.Avdeyev, et al. Physics of Atomic Nuclei, **64** (2001) 1549.
S.P.Avdeyev, et al. Phys.Letters, **B503** (2001) 256.

12. O.Shapiro, D.H.E.Gross. Nucl.Phys., **A573** (1994) 143.

13. V.Lips, et al. Phys.Lett., **B338** (1994) 141.

14. S.Y.Shmakov, et al. Yad.Fiz., **58** (1995) 1735;
Phys. of Atomic Nucl., **58** (1995) 1635.

15. V.A.Karnaukhov, et al. Preprint JINR, E7–98–8, Dubna, 1998;
Phys. of Atomic Nuclei, **62, N 2** (1999) 237.

16. M.Louvel, et al. Nucl.Phys., **A559** (1993) 137.

17. J.Pochodzalla. GSI Report 91–11, (1991).

18. D.Fox, et al. Phys.Rev., **C47** (1993) R421.

19. T.C.Sangster, et al. Phys.Rev., **C47** (1993) R2457.

20. B.Kampfer, et al. Phys.Rev., **C48** (1993) R955.

21. Zhi Yong He, et al. Nucl.Phys., **A620** (1997) 214.

22. G.Wang, et al. Phys.Rev., **C57** (1998) R2786.

23. D.Durand. Nucl.Phys., **A630** (1998) 52 c.

24. S.P.Avdeyev, et al. Nucl.Instrum.Meth., **A332** (1993) 149;
S.P.Avdeyev, et al. Pribory i Tekhnika Eksper., **39** (1996) 7;
(Instr.Exp.Techn., **39** (1996) 153).

25. J.Bondorf, et al. Phys.Rep., **257** (1995) 133;
A.S.Botvina, A.S.Iljinov, I.N.Mishustin. Nucl.Phys., **A507** (1990) 649;
A.S.Botvina, et al. Phys. of Atomic Nuclei, **57** (1994) 628.

26. V.D.Toneev, et al. Nucl.Phys., **A519** (1990) 463.

27. N.S.Amelin, et al. Yad.Fiz., **52** (1990) 272.
(Translated as Sov.Journ. of Nuclear Phys., **52** (1990) 172).

28. W.A.Friedman. Phys.Rev., **C42** (1990) 667.

29. L.Beaulieu et al. Phys.Rev.Lett., **84** (2000) 5971.

30. P.G.Akishin, I.V.Puzynin, S.I.Vinitsky. Comp.Math.Applic., **34**, No 2–4 (1997) 45.

Received by Publishing Department
on July 30, 2001.

Родионов В.К. и др. E1-2001-157

Временная шкала тепловой мультифрагментации
в соударениях $p+\mathrm{Au}$ при энергии 8,1 ГэВ

Изучена корреляция по относительному углу для фрагментов промежуточной массы (ФПМ), возникающих в соударениях $p+\mathrm{Au}$ при энергии 8,1 ГэВ. Наблюдается сильное подавление выхода совпадающих ФМП при малых относительных углах, обусловленное их кулоновским отталкиванием. Экспериментальная корреляционная функция сопоставляется с теоретическими значениями, полученными путем расчетов многотельных кулоновских траекторий для различных значений τ — среднего времени жизни фрагментирующей системы. Начальные условия для расчета (заряды, массы фрагментов, их координаты и тепловые скорости) находятся с помощью комбинированной модели, включающей модифицированный внутриядерный каскад с последующим применением статистической модели мультифрагментации. Тщательно исследована модельная зависимость результатов. Установлено, что среднее время распада фрагментирующего ядра $\tau \leq 70$ фм/с.

Работа выполнена в Лаборатории ядерных проблем им. В.П.Джелепова ОИЯИ.

Препринт Объединенного института ядерных исследований. Дубна, 2001

Rodionov V.K. et al. E1-2001-157

Time Scale of the Thermal Multifragmentation
in $p+\mathrm{Au}$ Collisions at 8.1 GeV

The relative angle correlation of intermediate mass fragments has been studied for $p+\mathrm{Au}$ collisions at 8.1 GeV. Strong suppression at the small angles is observed caused by IMF-IMF Coulomb repulsion. Experimental correlation function is compared to that obtained by the multi-body Coulomb trajectory calculations with the various decay times τ of fragmenting system. The combined model including the empirically modified intranuclear cascade followed by statistical multifragmentation was used to generate starting conditions for these calculations. The model dependence of the results obtained has been carefully checked. The mean decay time of fragmenting system is found to be $\tau \leq 70$ fm/c.

The investigation has been performed at the Dzhelepov Laboratory of Nuclear Problems, JINR.

Preprint of the Joint Institute for Nuclear Research. Dubna, 2001

Макет Н.А.Киселевой

Подписано в печать 05.09.2001
Формат 60 × 90/16. Офсетная печать. Уч.-изд. л. 1,5
Тираж 400. Заказ 52849. Цена 1 р. 50 к.

Издательский отдел Объединенного института ядерных исследований
Дубна Московской области